Journal of the Optical Society of Korea
Vol. 18, No. 1, February 2014, pp. 60-64
DOI: http://dx.doi.org/10.3807/JOSK.2014.18.1.060

Diffraction-Limited High-Power Single-Cycle Terahertz Pulse Generation in Prism-Cut $LiNbO_3$ for Precise Terahertz Applications

In Hyung Baek[1], Bong Joo Kang[1], Young Uk Jeong[2], and Fabian Rotermund[1]*

[1]*Department of Physics and Division of Energy Systems Research, Ajou University, Suwon 443-749, Korea*
[2]*Center for Quantum-Beam based Radiation Research, Korea Atomic Energy Research Institute, Daejeon 305-353, Korea*

(Received October 10, 2013 : revised January 2, 2014 : accepted January 20, 2014)

We report the generation of 3.3-mW single-cycle terahertz (THz) pulses at 1-kHz repetition rate via optical rectification in MgO-doped prism-cut stoichiometric $LiNbO_3$. Efficient pulse-front tilting of 800-nm pulses was realized by an optimized single-lens focusing scheme for radially-symmetric propagation of THz beams. In this geometry, nearly-diffraction-limited THz Gaussian beams with electric field strength as high as 350 kV/cm were generated. The pump-to-THz energy conversion efficiency of 1.36×10^{-3} and the extremely high signal-to-noise ratio of ~1:15000 achieved are among the best results for 1-kHz single-cycle terahertz pulse generation ever demonstrated in room temperature operation.

Keywords : Terahertz wave generation, Lithium niobate, Optical rectification
OCIS codes : (190.7110) Ultrafast nonlinear optics; (130.3730) Lithium niobate; (300.6495) Spectroscopy, terahertz

I. INTRODUCTION

Ultrashort electromagnetic radiation in the frequency region between 0.1 and 10 THz is of great interest for a variety of applications, such as optical spectroscopy, biomedical imaging, communications, and security systems [1-3]. In particular, studies on terahertz (THz) nonlinear phenomena in various materials, often require intense ultrashort THz pulses with microjoule-level energy and electric field strength of >100 kV/cm, are currently regarded as an unexplored new research area [4-7]. Since the availability of compact high-power ultrashort THz sources is quite limited yet, development of such sources is an essential step for advanced nonlinear spectroscopy and applications in the THz frequency range. There are different methods to generate ultrashort THz pulses depending on the desired frequency range and the purpose of applications. Thanks to both technical advances in femtosecond laser systems and photoconductive (PC) antennas based on semiconductor materials, several generation techniques are well-established for single-cycle THz pulse generation in the frequency range around 1 THz. The PC antenna-based THz emitters are widely used for THz time-domain spectroscopy (THz-TDS) to find molecular fingerprints of matters and to extract their optical constants [8]. Although such THz-TDS systems exhibit an excellent signal-to-noise ratio (SNR, ratio of the peak-to-peak signal amplitude and the root-mean-square noise amplitude) of >100000:1 in the temporal THz waveform [9], achievable THz pulse energies are limited and cannot exceed 1 μJ because of the limited illumination of excitation pulses on the PC antenna [10]. In last decade, optical rectification in second-order nonlinear optical crystals, such as ZnTe, GaSe, and DAST, has been emerging as an efficient alternative method for generating more intense single-cycle THz pulses. However, the magnitude of the THz pulse energy is often limited by several factors, such as absorption, phonon resonances, and photorefractive damages in nonlinear crystals [11, 12]. In addition, the group velocity of the ultrashort optical excitation pulses has to be well-matched to the phase velocity of the newly generated THz pulses in the nonlinear medium for efficient frequency conversion [13].

Lithium niobate ($LiNbO_3$) is a well-known nonlinear optical crystal and a potential candidate for efficient THz

*Corresponding author: rotermun@ajou.ac.kr
Color versions of one or more of the figures in this paper are available online.

wave generation due to its large second-order nonlinear coefficient (d_{eff} = 168 pm/V). The relatively large band-gap (E_g = 3.8 eV) of $LiNbO_3$ allows us to use near-infrared excitation sources without two-photon absorption [14]. However, the large index dispersion and mismatch in $LiNbO_3$ inhibit efficient phase matching in a collinear geometry. Since Hebling *et al.* suggested a non-collinear phase matching in a prism-cut $LiNbO_3$ using a tilted pulse-front pumping (TPFP) scheme and reported its proof-of-principle experiment for efficient THz pulse generation in 2003, many efforts have followed to improve both THz pulse energy and spectral bandwidth by utilizing different configurations and excitation sources [15-17]. As a result, it turned out that there was a tradeoff between the pump-to-THz conversion efficiency and the spectral bandwidth for THz pulse generation. It is not a trivial task to achieve simultaneously high-energy and broadband THz pulses via optical rectification, because the frequency conversion for high-frequency ranges of >3 THz is strongly limited by the low intensity distribution at both spectrum ends of the excitation pulses and the phase matching condition [18]. Up until now, most of activities dealing with this technique were focused on generation of high pump-to-THz conversion efficiency with moderate spectral bandwidths. Fülöp *et al.* reported sub-millijoule THz pulse generation based on a Yb:YAG amplifier system delivering 1.3-ps excitation pulses at 1030-nm wavelength and 10-Hz repetition rate. A high pump-to-THz energy conversion efficiency of 2.5×10^{-3} was achieved, but the spectral peak of the generated THz pulses was shifted to a quite low spectral range of 0.25 THz [19]. In addition, a low-repetition-rate THz system is not well-suited for applications in precise THz-TDS and nonlinear spectroscopy because of low SNR. Very recently, Huang *et al.* reported the highest pump-to-THz energy conversion efficiency of 3.8×10^{-2} by employing 1-kHz, 680-fs excitation pulses at 1030 nm. In this experiment, the prism-cut $LiNbO_3$ was cryogenically cooled down to 150 K in a dewar to reduce thermal loads and absorption behavior in $LiNbO_3$ [20]. In the present work, high-power single-cycle THz pulses with a diffraction-limited Gaussian profile were generated at room temperature by utilizing the TPFP technique at 800-nm wavelength. Although the previous study (Hirori et al. in [16]) demonstrated similar high-power THz pulse generation via TPFP, the 4f-lens arrangement led to an asymmetric propagation of the generated THz beam in vertical and horizontal directions. We adopt an optimized single-lens focusing geometry to generate radially-symmetric THz radiation from the prism-cut $LiNbO_3$ crystal. The system delivered a maximum average power of 3.3 mW, which corresponds to 3.3-μJ single pulse energy, and the highest SNR (~1:15000) ever achieved at 1-kHz repetition rate. A pump-to-THz energy conversion efficiency of 1.36×10^{-3} was obtained with 2.4-W pumping.

II. DESIGN OF EFFICIENT PHASE MATCHING BY TILTED PULSE-FRONT EXCITATION

For THz pulse generation, we used a 1-kHz Ti:sapphire regenerative amplifier (Spitfire Ace, Spectra Physics), delivering 4-W average output power with pulse duration of 100 fs at 800 nm, as the excitation source. Figure 1 shows the schematic configuration of a high-power THz pulse generation and detection system. This system can be further used for THz-TDS. The optical beam was divided by a 92:8 beam splitter for THz generation and detection.

The tilting angle (γ) of the pump pulse-front was controlled by an Au-coated diffraction grating (1800 grooves/mm) and a lens of 150-mm focal length using the following relation:

$$\tan\gamma = m\lambda_p / \left(d \cdot n_p^{group} \cdot \beta_1 \cdot cos\theta_d\right), \quad (1)$$

$$\tan\gamma = n_p^{group} \cdot \beta_2 \cdot tan\theta_d, \quad (2)$$

where m is the diffraction order, λ_p is the pump wavelength, d is the grating groove number, n_p^{group} is the group index of the pump pulse, β_1 and β_2 are the magnification factors of the lens for the pump wave front and the grating image, respectively, and θ_d is the diffraction angle [16]. To optimize the efficiency of THz pulse generation, we chose two magnification factors ($\beta_1 = \beta_2 \approx 0.591$) and the diffraction angle ($\theta_d = 56.1°$) by using the Eqs. (1) and (2), and the grating equation. After passing through a half-wave plate, the vertically-polarized excitation beam was focused on the 1.3-mol% MgO-doped prism-cut stoichiometric $LiNbO_3$ crystal with a dimension of 9×9×9 mm^3 by a single spherical lens with 150-mm focal length. Such

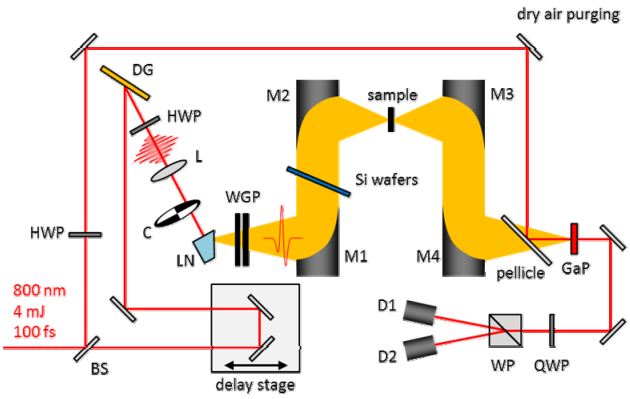

FIG. 1. Experimental setup for single-cycle THz pulse generation by tilted pulse-front excitation. BS: beam splitter, HWP: half-wave plate, DG: diffraction grating, L: convex lens, C: optical chopper, LN: 1.3-mol% MgO-doped prism-cut stoichiometric $LiNbO_3$ crystal, WGP: wire grid polarizers, M1-M4: metal-coated off-axis parabolic mirrors, QWP: quarter-wave plate, WP: Wollaston prism, D1 & D2: photo-detectors.

single-lens focusing geometry makes wave front images of the tilted pulse and the diffraction grating flat inside $LiNbO_3$ without distortion [14]. The incident facet of $LiNbO_3$ crystal was cut under an angle of 63° that can be calculated from the relation

$$v_{opt}^{group} \cdot cos\gamma = v_{THz}^{phase}. \quad (3)$$

The horizontal (d_H^I) and the vertical diameters (d_V^I) of the pump beam at the entrance-facet of crystal were 4 and 9 mm, respectively. The THz pulses generated were subsequently guided with four off-axis parabolic mirrors of different focal lengths to the detection stage. The average power of the THz pulses was measured by using a calibrated pyro-electric detector (THZ5B-MT-DZ, Gentec-EO) and the time trace of the THz electric field was recorded by an electro-optic sampling method in a 0.3-mm-thick GaP crystal. Six Si wafers were used to suppress the nonlinear response in the electro-optic sampling. The THz beam profile at focus was measured by using a pyroelectric camera (Pyro CAM-III, OPHIR). All of the measurements were carried out under dry air purging at room temperature of 20℃.

III. EXPERIMENTAL RESULTS

Figure 2 shows the generated THz average power versus the incident pump power, measured at the sample position of Fig. 1. The THz average power increased quadratically with increasing pump power. Above pump powers of 800 mW, the experimental data began to deviate slightly from the square-law curve (solid line). This might be mainly caused by the occurrence of free carrier absorption of THz pulses in $LiNbO_3$ [19]. In the pulse-front-tilted excitation scheme with combination of grating-lens-$LiNbO_3$, we were able to generate intense THz pulses with average powers up to 3.3 mW with 2.4-W pumping. Once the pump power exceeded 2.45 W, the photorefractive effect was observed in the crystal and this led to a slight decrease of the conversion efficiency. At a pump power of 2.4 W, the pump-to-THz energy conversion efficiency of 1.36×10^{-3} was obtained and the corresponding photon conversion efficiency was evaluated to be 74.8% by taking into account the peak frequency of 0.62 THz.

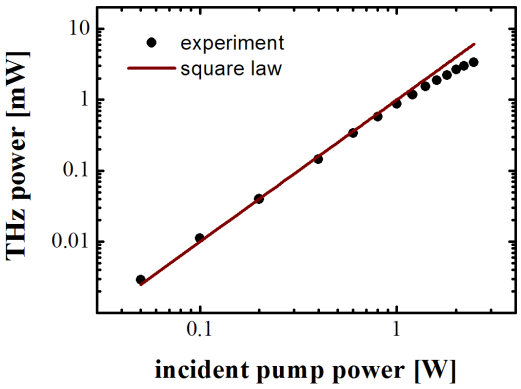

FIG. 2. Generated THz average power versus incident pump power (dots) and square law curve (solid).

Figure 3 shows the time trace of the generated THz pulses measured at the maximum average power by electro-optic sampling and the corresponding spectrum was obtained by fast Fourier transform (FFT). The THz electric field strength is given by

$$E_{THz} = \left(sin^{-1}((I_a - I_b)/(I_a + I_b)) \cdot \lambda_{opt}\right) / \left(2\pi \cdot n_{opt}^3 \cdot r_{41} \cdot t_{Si}^6 \cdot t_{GaP} \cdot l\right), \quad (4)$$

where I_a and I_b denote the signal amplitudes measured by two separate detectors. n_{opt} and r_{41} are the optical refractive index at 800 nm and the electro-optic coefficient of GaP, respectively. Furthermore, t_{si} and t_{GaP} are the Fresnel transmission coefficients of Si wafer and GaP, and l is the thickness of GaP [21]. As can be seen in the temporal profile of the THz pulse in Fig. 3(a), the peak-to-peak electric field strength amounted to 350 kV/cm, which was

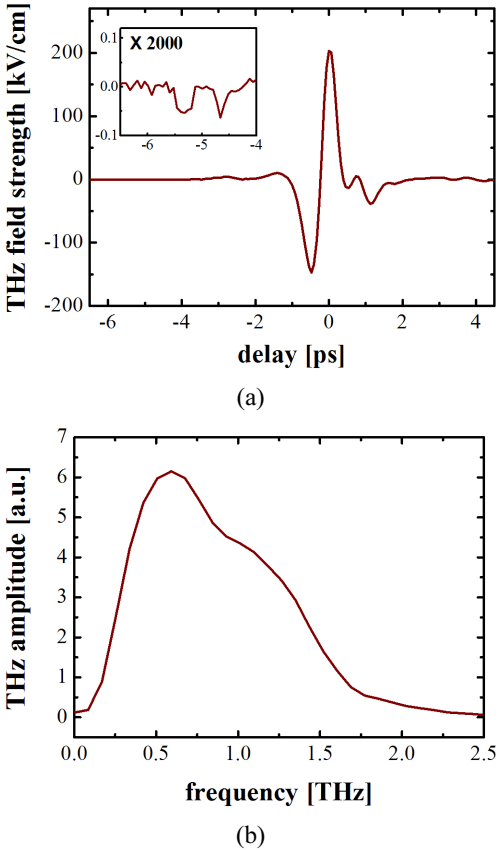

FIG. 3. Characteristics of single-cycle THz pulse. (a) Temporal profile of the THz pulse measured by electro-optic sampling and the 2000-fold magnification of the leading edge of the temporal THz waveform in y-axis (inset) and (b) the corresponding spectrum obtained by fast Fourier transform.

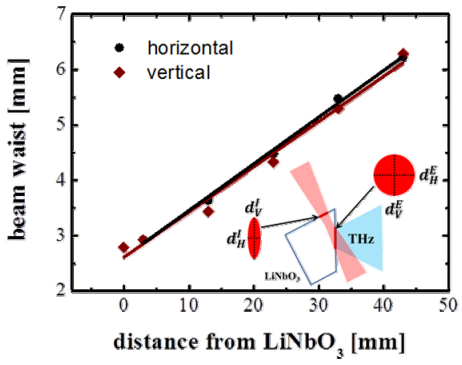

(a)

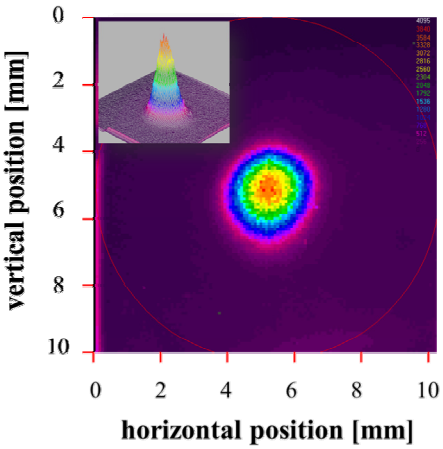

(b)

FIG. 4. (a) Spot size of the THz beam versus propagation distance from the emitter (inset: pump beam shape at entrance and exit facets) and (b) spatial beam profile of the THz beam at focal point between the parabolic mirrors M2 and M3.

calculated with $n_{opt} = 3.2$, $r_{41} = 0.88\,pm/V$, $t_{Si} = 0.523$, $t_{GaP} = 0.46$, and $l = 0.3\,mm$ taking into account the reflectivity of parabolic mirrors. The inset of Fig. 3(a) shows a 2000-fold-magnified feature of the leading edge in the temporal THz waveform. We obtained a SNR as high as ~1:15000 with a time constant of 300 ms when six Si attenuators were used. It is noted that this value is, to our knowledge, the highest one ever achieved with a THz system operating at 1-kHz repetition rate. Figure 3(b) shows the corresponding FFT spectrum. The center frequency and the spectral bandwidth were measured to be 0.62 THz and 1.1 THz, respectively. The water absorption, which usually occurs in this THz spectral region, could be almost suppressed by dry air purging.

An optimal focal length of the first parabolic mirror M1 was chosen through the measurement of the THz beam divergence. As shown in Fig. 4(a), the THz beam radius from the emitter to far-field was evaluated by the knife-edge method. We found that the radially-symmetric radiation of THz beams could be easily achieved by the optimized single-lens focusing scheme. As shown in inset of Fig. 4(a) and Eq. (5), the horizontal diameter (d_H^E=8.83 *mm*) of

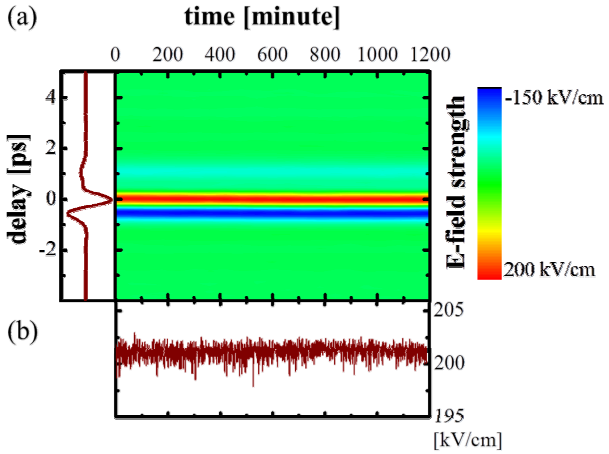

FIG. 5. Long-term stability of high-power THz wave generation system, measured for 20 hours. (a) THz electric field distribution and (b) the recorded peak value of the electric field as function of the operation time.

the pump beam projected at the exit-facet nearly equals the vertical diameter (d_V^E) of the pump beam at the same facet.

$$d_H^E = d_H^l/\cos(\gamma) \qquad d_V^E \approx d_V^l \tag{5}$$

The half divergence angles of the THz beam at the horizontal and vertical direction were measured to be 82.54 and 81.32 mrad, respectively.

Figure 4(b) shows the spatial intensity distribution of the THz beam at the focal point between the parabolic mirrors M2 and M3. The radial symmetric cross-section of the THz beam spot with a diameter of about 2 mm is clearly captured by the pyroelectric camera. The M^2-factor of 1.2 measured at this position implied that the generated THz beam exhibits a nearly diffraction-limited Gaussian profile.

Figure 5 shows the measured long-term stability of our THz pulse generation system. The time-trace of the THz electric field strength was recorded during 20 hours. Neither phase shift nor temporal distortion of the electric field was observed in the THz waveform. The peak value of the electro-optic sampling signal was also measured for the same period with N = 6000 sampling. The mean value of the electric field at the maximum with a standard deviation was estimated to be 201.1±0.6 kV/cm, which corresponds to an error of only < 0.3%. Finally, we could achieve an exceptionally high SNR of about 1:15000.

IV. CONCLUSIONS

We demonstrated efficient THz pulse generation in a prism-cut $LiNbO_3$ via optical rectification based on TPFP at 800 nm. It was shown that our THz generation system can generate 3.3-mW THz pulses with electric field strength

as high as 350 kV/cm and the pump-to-THz energy conversion efficiency of 1.36×10^{-3} at room temperature. We expect that such a high-power THz pulse generation system delivering nearly diffraction-limited 1-kHz THz pulses with extremely high signal-to-noise ratio (~1:15000) is very well suited for sensitive and precise THz applications in nonlinear and time-domain spectroscopy, imaging, and metrology.

ACKNOWLEDGMENT

This work was supported by National Research Foundation (NRF) funded by the Korean Government (MEST) (2011-0017494) and by the World Class Institute (WCI) program of NRF by MEST (WCI 2011-001).

REFERENCES

1. Y. Ueno and K. Ajito, "Analytical terahertz spectroscopy," Anal. Sci. **24**, 185-192 (2008).
2. E. Jung, M. Lim, K. Moon, Y. Do, S. Lee, H. Han, H. J. Choi, K.-S. Cho, and K.-R. Kim, "Terahertz pulse imaging of micro-metastatic lymph nodes in early-stage cervical cancer patients," J. Opt. Soc. Korea **15**, 155-160 (2011).
3. H.-J. Song and T. Nagatsuma, "Present and future of terahertz communications," IEEE Trans. THz Sci. Technol. **1**, 256-263 (2012).
4. M. C. Hoffmann, N. C. Brandt, H. Y. Hwang, K.-L. Yeh, and K. A. Nelson, "Terahertz Kerr effect," Appl. Phys. Lett. **95**, 231105 (2009).
5. F. H. Su, F. Blanchard, G. Sharma, L. Razzari, A. Ayesheshim, T. L. Cocker, L. V. Titova, T. Ozaki, J.-C. Kieffer, R. Morandotti, M. Reid, and F. A. Hegmann, "Terahertz pulse induced intervalley scattering in photoexcited GaAs," Opt. Express **17**, 9620-9629 (2009).
6. E. Hendry, P. J. Hale, J. Moger, and A. K. Savchenko, "Coherent nonlinear optical response of graphene," Phys. Rev. Lett. **105**, 097401 (2010).
7. K. Tanaka, H. Hirori, and M. Nagai, "THz nonlinear spectroscopy of solids," IEEE Trans. THz Sci. Technol. **1,** 301-312 (2011).
8. D. Grischkowsky, S. Keiding, M. van Exter, and Ch. Fattinger, "Far-infrared time-domain spectroscopy with terahertz beams of dielectrics and semiconductors," J. Opt. Soc. Am. B **7**, 2006-2015 (1990).
9. I. Kostakis, D. Saeedkia, and M. Missous, "Terahertz generation and detection using low temperature grown InGaAs-InAlAs photoconductive antennas at 1.55 μm pulse excitation," IEEE Trans. THz Sci. Technol. **2,** 617-622 (2012).
10. D. You, R. R. Jones, P. H. Bucksbaum, and R. Dykaar, "Generation of high-power sub-single-cycle 500-fs electromagnetic pulses," Opt. Lett. **18**, 290-292 (1993).
11. A. Schneider, M. Neis, M. Stillhart, B. Ruiz, R. U. A. Khan, and P. Günter, "Generation of terahertz pulses through optical rectification in organic DAST crystals: Theory and experiment," J. Opt. Soc. Am. B **23**, 1822-1835 (2006).
12. J. R. Schwesyg, M. Falk, C. R. Phillips, D. H. Jundt, K. Buse, and M. M. Fejer, "Pyroelectrically induced photorefractive damage in magnesium-doped lithium niobate crystals," J. Opt. Soc. Am. B **28**, 1973-1987 (2011).
13. L. Xu, X.-C. Zhang, and D. H. Auston, "Terahertz beam generation by femtosecond optical pulses in electro-optic materials," Appl. Phys. Lett. **61**, 1784-1786 (1992).
14. J. A. Fülöp, L. Pálfalvi, G. Almási, and J. Hebling, "Design of high-energy terahertz sources based on optical rectification," Opt. Express **18**, 12311-12317 (2010).
15. A. G. Stepanov, L. Bonacina, S. V. Chekalin, and J.-P. Wolf, "Generation of 30 μJ single-cycle terahertz pulses at 100 Hz repetition rate by optical rectification," Opt. Lett. **33**, 2497-2499 (2008).
16. H. Hirori, A. Doi, F. Blanchard, and K. Tanaka, "Single-cycle terahertz pulses with amplitudes exceeding 1 MV/cm generated by optical rectification in $LiNbO_3$," Appl. Phys. Lett. **98**, 091106 (2011).
17. S. B. Bodrov, I. E. Ilyakov, B. V. Shishkin, and A. N. Stepanov, "Efficient terahertz generation by optical rectification in Si-$LiNbO_3$-air-metal sandwich structure with variable air gap," Appl. Phys. Lett. **100**, 201114 (2012).
18. X.-C. Zhang and J. Xu, *Introduction to THz Wave Photonics* (Springer, New York, USA, 2010), pp. 28-30.
19. J. A. Fülöp, L. Pálfalvi, S. Klingebiel, G. Almási, F. Krausz, S. Karsch, and J. Hebling, "Generation of sub-mJ terahertz pulses by optical rectification," Opt. Lett. **37**, 557-559 (2012).
20. S.-W. Huang, E. Granados, W. R. Huang, K.-H. Hong, L. E. Zapata, and F. X. Kärtner, "High conversion efficiency, high energy terahertz pulses by optical rectification in cryogenically cooled lithium niobate," Opt. Lett. **38**, 796-798 (2013).
21. Q. Wu and X.-C. Zhang, "Free-space electro-optics sampling of mid-infrared pulses," Appl. Phys. Lett. **71**, 1285-1286 (1997).